Separation Science and Technology
Publication details, including instructions for authors and subscription information:
http://www.informaworld.com/smpp/title~content=t713708471

A New Type of Hollow-Fiber Pertractor

Štefan Schlosser[a]; Iveta Rothová[a]
[a] DEPARTMENT OF CHEMICAL AND BIOCHEMICAL ENGINEERING, SLOVAK TECHNICAL UNIVERSITY RADLINSKÉ, BRATISLAVA, SLOVAKIA

To cite this Article Schlosser, Štefan and Rothová, Iveta(1994) 'A New Type of Hollow-Fiber Pertractor', Separation Science and Technology, 29: 6, 765 — 780
To link to this Article: DOI: 10.1080/01496399408005607
URL: http://dx.doi.org/10.1080/01496399408005607

SEPARATION SCIENCE AND TECHNOLOGY, **29**(6), pp. 765–780, 1994

A New Type of Hollow-Fiber Pertractor*

ŠTEFAN SCHLOSSER and IVETA ROTHOVÁ
DEPARTMENT OF CHEMICAL AND BIOCHEMICAL ENGINEERING
SLOVAK TECHNICAL UNIVERSITY
RADLINSKÉHO 9, 812 37 BRATISLAVA, SLOVAKIA

ABSTRACT

The performance of a new hollow-fibers-in-tube type pertractor has been studied. This pertractor consists of a hydrophilic tube in which a bundle of hydrophobic hollow fibers is inserted. An *n*-alkane fraction was used as the membrane phase. Pulsation of this phase increases the mass flux by more than 40% at a relatively low pulse velocity and reaches a maximum value at about 10 $mm \cdot s^{-1}$. Wettability of the microporous walls plays an important role. A substantially higher mass flux, by about 60%, can be reached when the stripping solution is in contact with the hydrophilic wall. Analysis of the mass-transfer resistances has revealed that the main resistance is found in the liquid membrane phase, especially in the phase soaked into the hydrophobic pores. The values of the mass flux per unit volume of the pertractor ranged from 9 to 20 $mol \cdot m^{-3} \cdot h^{-1}$. These values are much higher than those obtained with other bulk and supported liquid membranes and are comparable with emulsion-type liquid membranes.

INTRODUCTION

Microporous walls, mostly in the form of hollow fibers, have been used for the immobilization of interfaces in solvent extraction or absorption (1–4). Recently, contactors-pertractors with bulk liquid membranes were developed for separations in three-phase systems (5–9). Hollow-fiber pertractors have been used for separation of liquid solutions (5–7) and gases. A spiral-wound pertractor has been studied (9). Usually two bundles of

* Presented at the 4th World Congress of Chemical Engineering, Karlsruhe, Germany, June 16–21, 1991, as Paper 10.2-5.

hollow fibers with microporous walls are placed in a cylinder with solvent between the fibers. Mass transfer from one bundle to another occurs. Thus, a large interfacial area can be formed without the need for mechanical dispersion; this is advantageous for systems with an emulsion-forming tendency. The influence of porous wall wettability on mass transfer in two-phase systems has been investigated (2, 10, 11).

Mass transfer in a new pertractor of the hollow-fibers-in-a-tube type was studied.

THEORETICAL

A pertractor is formed by two types of porous walls, hydrophilic and hydrophobic, as shown schematically in Fig. 1. At least five characteristic liquid layers can be differentiated in this three-phase system. The concentration profile of the permeant in a pertractor with the feed flowing along the hydrophilic wall and the stripping solution in contact with the hydrophobic wall is schematically drawn in Fig. 2. Mass transfer in a stagnant bulk membrane phase and in phases soaked in pores occurs by molecular diffusion. In the pertraction of weak acids, only undissociated acid molecules, whose concentration in the aqueous solution is given by the relation

$$\frac{C}{C_a} = \frac{1}{1 + K_a \times 10^{pH}} \tag{1}$$

are transported through the membrane. The rate equations for the steady-

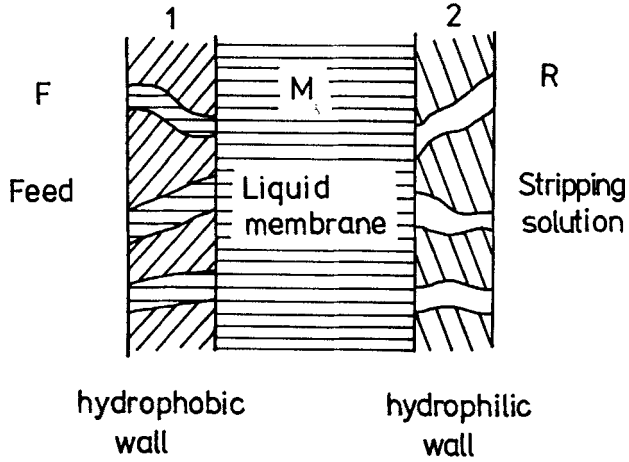

FIG. 1 Schematic of the three-phase system in a pertractor with two immobilized interfaces using microporous walls of different wettabilities.

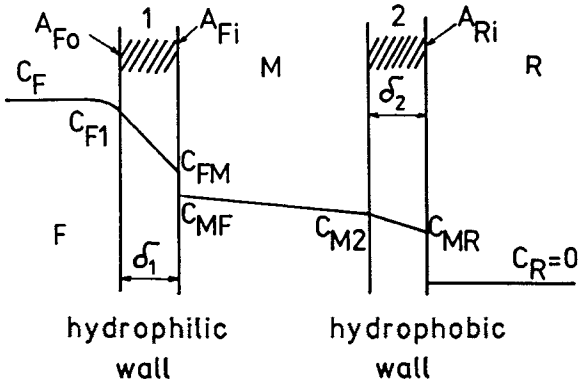

FIG. 2 Concentration profile of the permeant in a pertractor with the hydrophilic wall on the feed side (mode PV1-1 or 3, for $m_F < 1$).

state flux in a sufficiently short part of a pertractor with the configuration displayed in Fig. 2 can be written as

$$\dot{N} = KA_1\epsilon_1(C_F - C_R) \tag{2}$$

$$\dot{N} = k_F A_{Fo}(C_F - C_{F1}) \tag{3}$$

$$\dot{N} = k_1 A_1 \epsilon_1 (C_{F1} - C_{FM}) \tag{4}$$

$$\dot{N} = k_M A_M (C_{MF} - C_{M2}) \tag{5}$$

$$\dot{N} = k_2 A_2 \epsilon_2 (C_{M2} - C_{MR}) \tag{6}$$

An instantaneous neutralization reaction at the membrane-stripping solution interface along with a sufficiently high stoichiometric excess of reactant (NaOH) in the stripping solution were assumed. These presumptions resulted in zero resistance in the stripping solution because the concentration of undissociated permeant molecules in the strip was zero.

For the equilibrium at the feed–membrane interface, the following relation is valid:

$$C_{MF} = m_F C_{FM} \tag{7}$$

For the overall mass-transfer resistance, the following relations

$$\frac{1}{K} = \frac{A_1\epsilon_1}{k_F A_{Fo}} + \frac{1}{k_1} + \frac{A_1\epsilon_1}{k_M A_M m_F} + \frac{A_1\epsilon_1}{k_2 A_2 \epsilon_2 m_F} \tag{8}$$

$$R = R_F + R_1 + R_M + R_2 \tag{9}$$

can be derived from Eqs. (2)–(7).

For the case where the feed flows along the hydrophobic wall and the stripping solution is in contact with the hydrophilic wall, the concentration profile of the permeant in the pertractor is schematically depicted in Figs. 1 and 3. In a similar way, one can develop an equation for the overall resistance against mass transfer:

$$\frac{1}{K} = \frac{A_1\epsilon_1}{k_F A_{Fi}} + \frac{1}{k_1 m_F} + \frac{A_1\epsilon_1}{k_M A_M m_F} \tag{10}$$

$$R = R_F + R_1 + R_M \tag{11}$$

It was assumed, as before, that the resistances in the stripping solution in both the hydrophilic wall pores and in the bulk liquid are zero.

The individual mass-transfer coefficients in the fluid phases can be estimated by using the nondimensional equation of type:

$$\frac{kd}{D} = A\left(\frac{dv}{\nu}\right)^{\alpha}\left(\frac{\nu}{D}\right)^{\beta}\left(\frac{d}{l}\right)^{\gamma} \tag{12}$$

Dahuron and Cussler (3) used the following relation for mass transfer in laminar flow inside hollow fibers:

$$\frac{kd}{D} = 1.5\left(\frac{d^2v}{lD}\right)^{1/3} \tag{13}$$

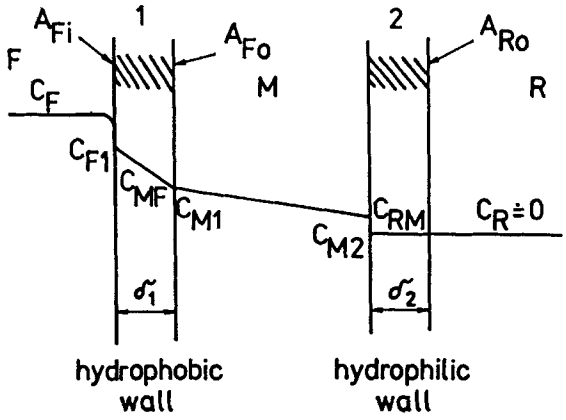

FIG. 3 Concentration profile of the permeant in a pertractor with the hydrophilic wall on the stripping solution side (mode PV1-4, $m_F < 1$).

and used

$$\frac{kd_e}{D} = 8.8\,\frac{d_e^2 v}{lv}\left(\frac{\nu}{D}\right)^{1/3} \tag{14}$$

for the flow around the fibers.

The individual mass-transfer coefficients for diffusional transport in stagnant liquids soaked into the pores of microporous walls are defined by

$$k_1 = D_1/\delta_1\tau_1, \qquad k_2 = D_2/\delta_2\tau_2 \tag{15}$$

where τ_1 and τ_2 are the tortuosities of the wall pores.

The mass flux in the pertractor can be described by

$$\dot{N} = \dot{V}_R(C_{aR} - C_{aRo}) \tag{16}$$

Combining Eqs. (2) and (16) for cases where both C_R and C_{aRo} have zero values, one obtains an equation for the overall mass-transfer coefficient:

$$K = \frac{\dot{V}_R C_{aR}}{A_1\epsilon_1 C_{Fm}} \tag{17}$$

The overall and the individual mass-transfer resistances can be calculated using Eqs. (8), (9) or (10), (11), respectively, depending on the mode of the pertractor operation. The resistance in the liquid membrane phase outside the wall pores can be estimated as

$$R_M = R - (R_F + R_1 + R_2) \tag{18}$$

where the value of R is based on experimental results, and R_F, R_1, and R_2 (if applicable) are calculated values.

EXPERIMENTAL

The properties of an *n*-alkane fraction (C_{10}, 5.4; C_{11}, 40.6; C_{12}, 40.4; and C_{13}, 13.1 wt%) used as the membrane phase include: mean molecular mass, 164.2 g·mol^{-1}; density (25°C), 0.743 g·cm^{-3}; kinematic viscosity (25°C), 1.66 × 10^{-6} m^2·s^{-1}. The aqueous feed contained 1 g·L^{-1} phenol and 0.1 M Na_2SO_4 with a pH of about 3.5. The stripping solution was aqueous 0.05 M NaOH, if not otherwise stated.

The equilibrium phenol concentrations were determined in temperature-controlled separatory funnels (25°C), shaken at least 4 hours to obtain equilibrium. The phenol distribution coefficient remained practically constant over the phenol concentration range in the aqueous phase from 300

to 1600 mg·L^{-1} at values of 0.104 and 0.118 for the system water/*n*-alkanes and for the aqueous solution containing 0.1 M Na_2SO_4/*n*-alkanes, respectively.

The phenol diffusion coefficient calculated using the Wilke–Chang's equation (12) had values of 9.98×10^{-10} and 1.416×10^{-10} m^2·s^{-1} at 25°C in water and *n*-alkanes, respectively.

A new pertractor (PV1) of the hollow-fiber-in-a-tube type, depicted in Fig. 4, was tested. A bundle of eight hollow fibers (Celgard X-10, Hoechst Celanese Corp.) was inserted into a polysulfone tubulet (Porofilt PS 10000, Tatabányai Szénbányák, Hungary) and glued with epoxy resin into a 4-mm inner diameter glass tube. The main characteristics of microporous hollow-fibers with mean pore diameters of 0.03 μm and of the ultrafiltra-

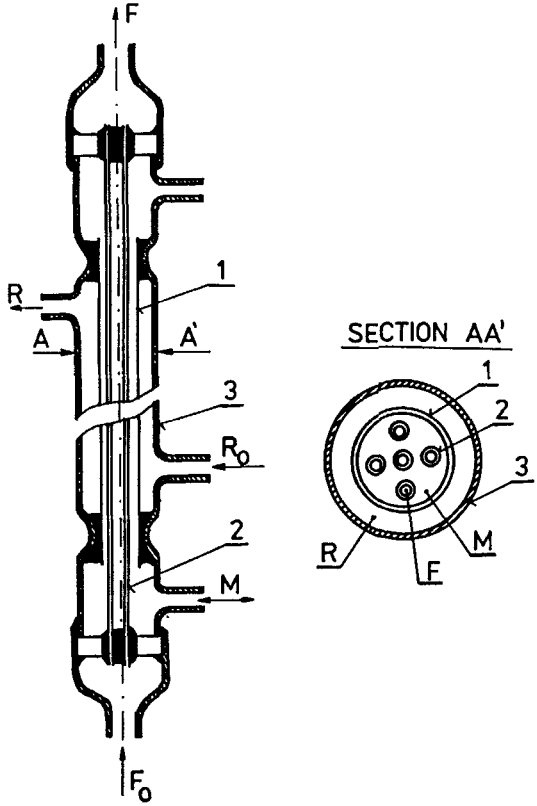

FIG. 4 Bulk liquid membrane pertractor PV1 of the hollow-fiber type in a tube (mode of operation PV1-4): 1 = tubular wall, 2 = hollow fiber, 3 = glass wall, F = feed, M = liquid membrane phase, R = stripping solution.

TABLE 1
Characteristics of Microporous Walls in the Module

	Celgard X-10, polypropylene (hydrophobic)	Porofilt PS 10000, polysulfone (hydrophilic)
Number of fibers (tubes)	8	1
Inner diameter, mm	0.20	1.43
Wall thickness, mm	0.025	0.16
Length (effective), mm	224	224
Porosity, %	20	70
Tortuosity of pores	1.9	1.4

tion tubulet membrane with a cut-off of about 10,000 Daltons are listed in Table 1. The outer and the inner diameters of the hollow fibers at both potted ends of the pertractor were measured with a microscopic comparator, and their mean values are summarized in Table 1. The porosity of the polysulfone tubulet was estimated from the dry and the wet weights of a plannar piece of the membrane (axially cutted and unfolded piece of tubulet) immersed in the feed solution for 24 hours. Tortuosity of the hollow-fiber pores was taken as 1.9, which is lower than that reported by Sengupta (7) and Prasad (4). For tortuosity values above 2, however, the sum of the calculated resistances ($R_F + R_1 + R_2$) is greater than the overall resistance estimated experimentally for cases with membrane phase pulsation, which is unrealistic. Tortuosity of the hydrophilic wall was calculated according to Wolf and Strieder (13).

The pertractor PV1 operated in two modes. In the first mode the feed flowed through the pertractor shell and the stripping solution flowed through the hollow fibers. This mode is shown in Fig. 5 and will be identified as PV1-1 and PV1-3. In the PV1-3 mode the feed was fed gravitationally (*not* by a piston pump) from a container (5) to avoid pulsations. In the PV1-4 mode the feed flowed through the hollow fibers and the stripping solution flowed through the shell, i.e., it was in contact with the hydrophilic wall, as shown in Figs. 1 and 4. The feed was supplied by a UNIPAN 335A piston pump. When the feed was in contact with the hydrophilic wall (mode PV1-1), the feed pulses were transferred into the membrane phase, which also pulsated but with a small amplitude, below 2.5 mm. In the case where the feed flowed through the hydrophobic hollow fibers (mode PV1-4), the pulses were not transferred into the membrane phase. The stripping solution was pumped by a Zalimp 315 peristaltic pump using Viton tubing. At the beginning of each experiment, the module was washed with all three phases. The run was subsequently carried out for at least 8 hours until steady state was reached.

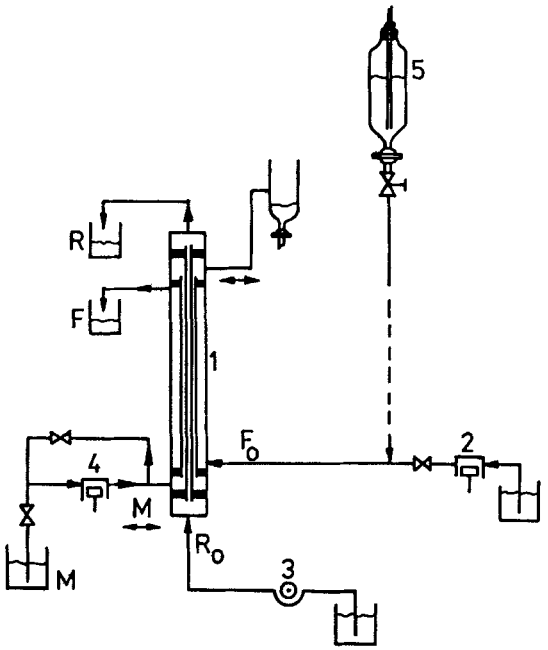

FIG. 5 The flow sheet of a bulk LM pertractor circuit (mode of operation PV1-1 or 3): 1 = pertractor (see Fig. 4), 2 = feed pump, 3 = stripping solution pump, 4 = membrane-phase pump (pulsator), 5 = container for gravitational dosage of the feed.

To study the influence of pulsations in more detail, the membrane phase pulsations were directly introduced by a piston pump in experiments of the PV1-4 mode. The suction and delivery side of the pump were connected to the pertractor chamber filled with the liquid membrane phase (Fig. 5). In most experiments the volume flow rates of the feed and of the stripping solution were maintained close to 1 and 0.37 $cm^3 \cdot min^{-1}$, respectively.

The concentration of phenol in the aqueous phase was estimated spectrophotometrically at a wavelength of 510 nm, using 4-aminoantipyrine as the color-forming reagent with phenol in $K_3[Fe(CN)_6]$ solution as the oxidation medium at a solution pH of 10 ± 0.2.

RESULTS AND DISCUSSION

Inspection of Figs. 6 and 7 reveals that the value of the overall mass-transfer coefficient is independent of the volume flow rates of both the feed and the stripping solution in hollow fibers. Although the experimental range of these flow rates was relatively narrow, one can suppose a similar

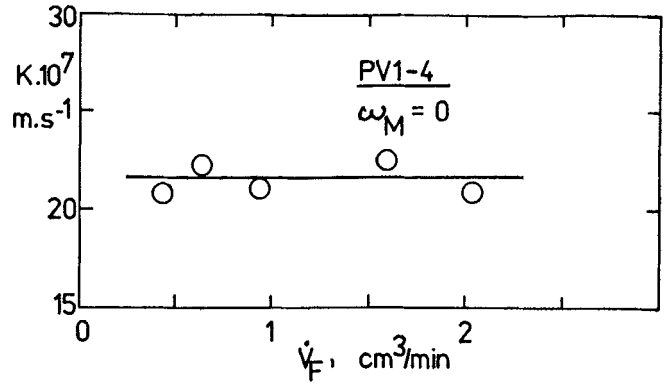

FIG. 6 The effect of the feed volumetric flow rate in hollow fibers on the overall mass-transfer coefficient ($\dot{V}_R$ = 0.36 cm·min^{-1}).

course over a broader range of values. The portion of the resistance due to mass transfer in the boundary layer of the feed compared to the overall resistance is small. Thus, any change caused by varying the feed volume flow affects the overall resistance, and accordingly the overall mass-transfer coefficient, only insignificantly. In the case of a stoichiometric excess of reagent, the resistance of the stripping solution is practically zero. In our experiments the phenol concentration in the stripping solution varied from 50 to 130 g·m^{-3}. These values correspond to a 94–130-fold excess of the reagent.

When the feed was flowing in the shell, i.e., along the hydrophilic membrane (mode of operation PV1-1 or 3), the pulsations caused by dosing

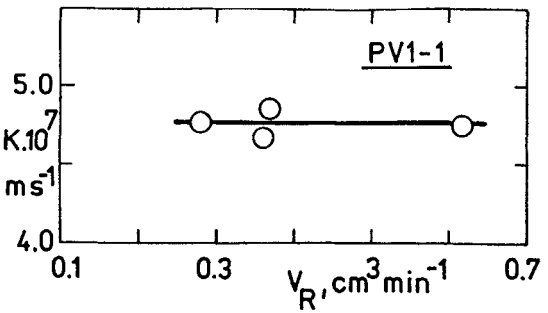

FIG. 7 The overall mass-transfer coefficient vs volumetric flow rate of the stripping solution in hollow fibers (ω_F = 20 min^{-1}, $\dot{V}_F$ = 0.92 cm^3·min^{-1}).

the feed were transmitted into the membrane phase with an amplitude smaller than 2.5 mm. This resulted in increases in both the overall mass-transfer coefficient and the mass flux through the membrane (Figs. 8 and 12). As shown in Figs. 9 and 12, direct pulsations of the membrane phase with a greater amplitude due to a piston pump increased the value of the overall mass-transfer coefficient, as well as the mass flux, by 40%. It is shown in Figs. 9 and 10 that the value of the overall mass-transfer coefficient increased when both the frequency and the amplitude of the pulsations were raised. Even at relatively low frequency and amplitude values, a maximum value of the overall mass-transfer coefficient was achieved. A useful quantity for evaluation of the influence of pulsations seems to be the pulse velocity (the product of ω_M and h). This enabled the data from both sets of measurements presented in Figs. 9 and 10 to be combined, as reported in Fig. 11. The pulse velocity is a quantity widely also used in pulsed extraction columns (14). Figure 11 clearly shows that even at a relatively low pulse velocity, i.e., 10 mm·s^{-1}, the maximum value of the mass-transfer coefficient was reached. Analysis of mass-transfer resistances revealed that the resistance in the bulk of the liquid membrane (outside of the wall pores), R_M, decreased with increasing pulse velocity and pulse frequency, as presented in Figs. 13 and 14.

It is evident from Fig. 12 that a substantially higher mass flux through the membranes can be reached when the stripping solution is in contact with the hydrophilic wall (mode PV1-4), i.e., when this solution fills the wall pores. In both modes of operation of pertractor PV1, the pores of

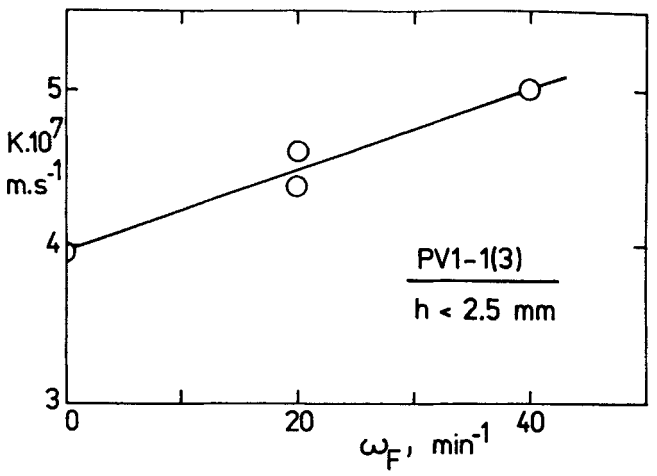

FIG. 8 The influence of pulse frequency in the feed on the overall mass-transfer coefficient.

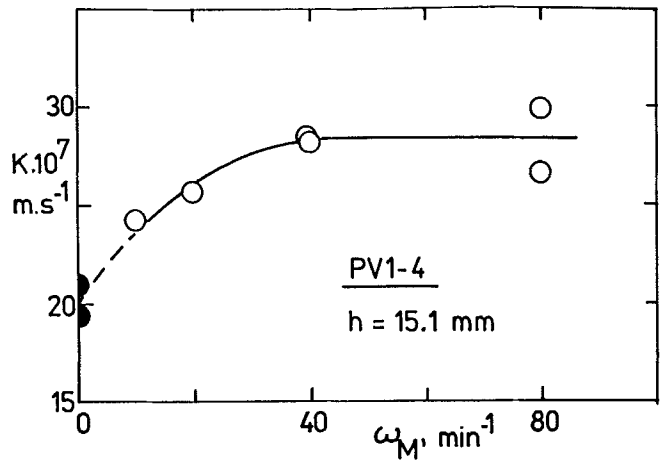

FIG. 9 The overall mass-transfer coefficient in pertractor PV1-4 vs pulse frequency of the membrane phase in PV1-4.

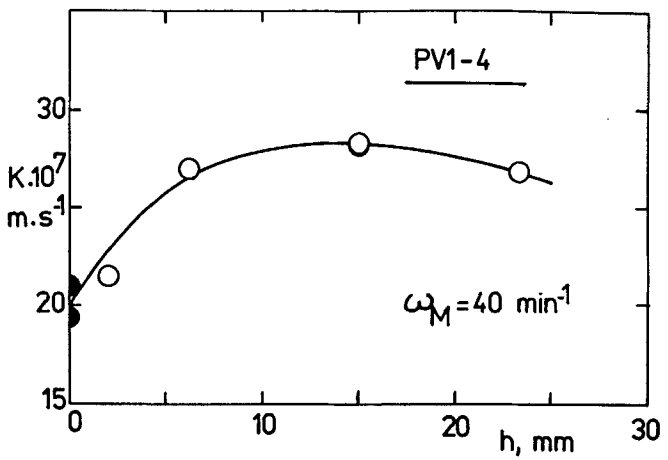

FIG. 10 The effect of the pulse amplitude on the overall mass-transfer coefficient in PV1-4.

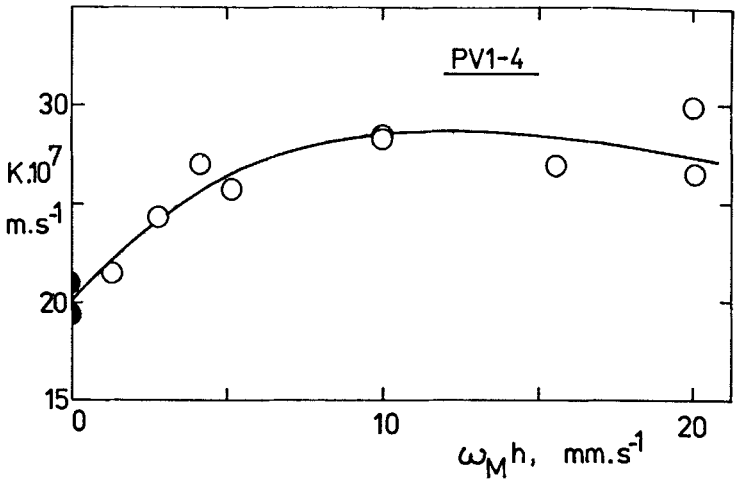

FIG. 11 The overall mass-transfer coefficient vs pulse velocity of the membrane phase in PV1-4.

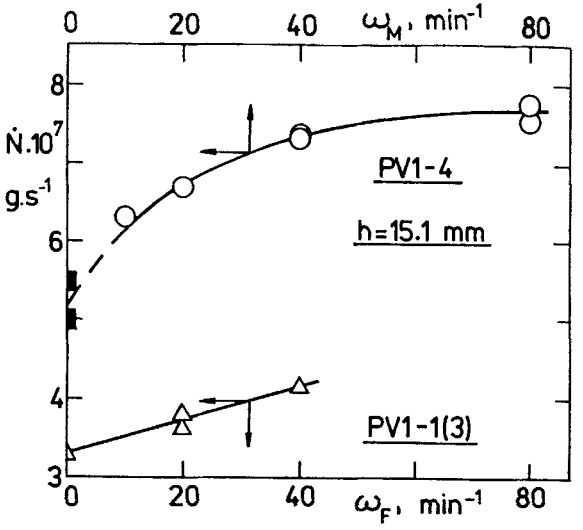

FIG. 12 The overall mass flux in the PV1 pertractor vs pulse frequencies.

the hydrophobic wall are filled with the membrane phase, and the main portion of resistance takes place in this wall. The overall driving force is practically the same and equal to C_F ($C_R = 0$). In the PV1-1 or 3 mode, as can be read from Fig. 12, the resistance in the wall on the stripping solution side is significant.

Analysis of mass-transfer resistances in individual phases and layers reveals that the main resistance is in the liquid membrane (R_1 and R_M in Fig. 13, and R_M and R_2 in Fig. 14). As the pulse velocity and/or the frequency of pulsations increases, the resistance of the bulk membrane (R_M) decreases as a result of the introduction of convective flow. R_M already has a small value for pulse velocities above 10 mm·s^{-1}. A more detailed analysis shows that the main resistance is located in the hydrophobic wall, i.e., in the liquid membrane soaked in its pores (Figs. 13 and 14), where mass transfer occurs only by molecular diffusion.

Starting from experimental values of the overall mass-transfer coefficients, values of the mass flux through liquid membranes per unit volume

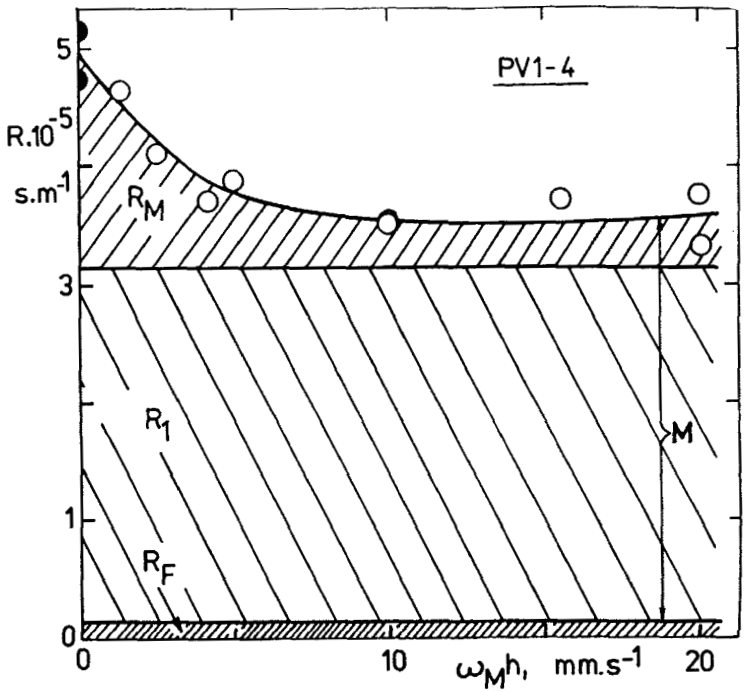

FIG. 13 The overall mass-transfer resistance and the resistances in various layers vs pulse velocity in PV1-4.

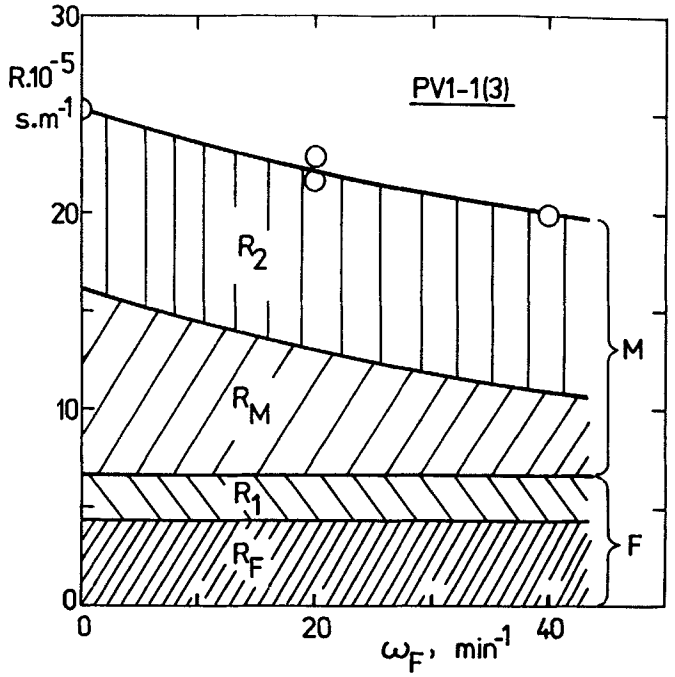

FIG. 14 The overall mass-transfer resistance and the resistances in various layers vs pulse frequency of the feed in PV1-1(3), $h < 2.5$ mm.

of the membrane module were calculated. An element of the pertractor with a cross section of 2.5 × 2.5 mm and a tubulet placed in the middle with an effective length as in PV1 were used for these calculations. Values of the mass flux per unit volume vary from 9 to 20 $mol \cdot m^{-3} \cdot h^{-1}$. The optimum value is several times higher than for other types of modules with bulk liquid membranes; 3.7 times larger than for supported liquid membranes and comparable with the fluxes of emulsion-type liquid membranes, based on published data (15, 16).

CONCLUSIONS

Pulsations of the membrane phase contribute substantially to enhancement of the mass-transfer rate in a hollow-fiber-in-tube-type pertractor. The wettability of microporous walls plays an important role. It is advantageous in the studied system to contact the stripping solution with the hydrophilic wall. The main part of the mass-transfer resistance is in the

liquid membrane phase; i.e., in the hydrophobic wall pores. The mass flux per unit volume of the contactor hollow-fiber-in-tube type is higher than in classical bulk liquid membrane contactors and comparable with supported and emulsion-type liquid membrane contactors.

NOTATION

A	surface area (m^2)
A_1, A_2	mean surface area of walls, $0.5(A_i + A_o)$ (m^2)
A_M	mean surface area in the bulk liquid membrane, $0.5(A_{Fi} + A_{Ro})$ and $0.5(A_{Fo} + A_{Ri})$ for PV1-1(3) and PV1-4, respectively (m^2)
C	concentration of the undissociated permeant molecules ($g \cdot m^{-3}$)
C_a	analytical (overall) concentration of the permeant ($g \cdot m^{-3}$)
C_{Fm}	mean concentration of the permeant in the feed, $0.5(C_{Fo} + C_F)$ ($g \cdot m^{-3}$)
d	diameter of the fiber or the tube (m)
d_e	equivalent diameter (4 cross sections/wetted perimeter) (m)
D	diffusion coefficient ($m^2 \cdot s^{-1}$)
h	amplitude of pulsation (m)
k	individual mass-transfer coefficient ($m \cdot s^{-1}$)
K	overall mass-transfer coefficient ($m \cdot s^{-1}$)
K_a	dissociation constant of weak acid (phenol)
l	length of the fiber or the tube (m)
m_F	distribution coefficient, Eq. (7)
$\dot{N}$	mass flux ($g \cdot s^{-1}$)
R	mass-transfer resistance ($s \cdot m^{-1}$)
v	velocity of flow ($m \cdot s^{-1}$)
$\dot{V}$	flow rate ($m^3 \cdot s^{-1}$)
δ	thickness of the microporous wall (m)
ϵ	wall porosity
ω	pulsation frequency (s^{-1})
$\omega_M h$	pulse velocity of the membrane phase ($m \cdot s^{-1}$)
τ	tortuosity of the wall pores
ν	kinematic viscosity ($m^2 \cdot s^{-1}$)

Indices

F	feed, feed–membrane interface
i	inner surface
M	liquid membrane outside of pores

o	outer surface
R	stripping solution
1	wall on the feed side
2	wall on the stripping solution side

ACKNOWLEDGMENTS

The support of Prof. E. Cussler from the University of Minnesota and Dr. R. W. Callahan from Hoechst Celanese Corp. in providing samples of Celgard fibers are gratefully acknowledged. We would also like to thank Dr. I. Zsirai from Tatabányai Banyák Vállalat, Hungary, for providing samples of Porofilt tubes. This work was supported by Grant 1/155/92 from the Ministry of Education and Science of Slovak Republic.

REFERENCES

1. R. Prasad and K. K. Sirkar, *Sep. Sci. Technol.*, *22*, 619 (1987).
2. R. Prasad and K. K. Sirkar, *AIChE J.*, *33*, 1057 (1987).
3. L. Dahuron and E. L. Cussler, *Ibid.*, *34*, 130 (1988).
4. R. Prasad and K. K. Sirkar, *Ibid.*, *34*, 177 (1988).
5. Y. Sato, K. Kondo, and F. Nakashio, *J. Chem. Eng. Jpn.*, p. 23 (1990).
6. A. Sengupta, R. Basu, R. Prasad, and K. K. Sirkar, *Sep. Sci. Technol.*, *23*, 1735 (1988).
7. A. Sengupta, R. Basu, and K. K. Sirkar, *AIChE J.*, *34*, 1698 (1988).
8. S. Majumdar, A. K. Guha, and K. K. Sirkar, *Ibid.*, *34*, 1135 (1988).
9. M. Teramoto, H. Matsuyama, H. Takaya, and T. Yonehara, *Proc. ISEC'88*, Vol. III, Moscow, July 1988, pp. 110–113.
10. R. Basu, R. Prasad, and K. K. Sirkar, *AIChE J.*, *36*, 450 (1990).
11. R. Prasad, S. Khare, A. Sengupta, and K. K. Sirkar, *Ibid.*, *36*, 1592 (1990).
12. R. C. Reid, J. M. Prausnitz, and T. K. Sherwood, *The Properties of Gases and Liquids*, 3rd ed., McGraw-Hill, New York, 1977, Chap. 11.
13. J. R. Wolf and W. Strieder, *J. Membr. Sci.*, *49*, 103 (1990).
14. T. C. Lo, M. M. Baird, and C. Hanson (Eds.), *Handbook of Solvent Extraction*, Wiley, New York, 1983, Chapters 11.1 and 11.2.
15. Š. Schlosser and E. Kossaczký, *J. Radioanal. Nuclear Chem., Articles*, *101*, 115 (1986).
16. Š. Schlosser, "Liquid Membranes—Theory and Practice," in *Advances in Membrane Phenomena and Processes* (lecture textbook of the ESMST Summer School, Gdansk-Sobieszewo, June 1988), Wroclaw Technical University Press, Wroclaw, Poland, 1989, p. 163.

Received by editor November 23, 1992
Revised June 10, 1993